

# Biomolecular Recognition Based on Single Gold Nanoparticle Light Scattering

G. Raschke,\* S. Kowarik, T. Franzl, C. Sönnichsen,<sup>†</sup> T. A. Klar, and J. Feldmann

*Photonics and Optoelectronics Group, Department of Physics and CeNS,  
Ludwig-Maximilians-Universität, Amalienstr. 54, D-80799 Munich, Germany*

A. Nichtl and K. Kürzinger

*Roche Diagnostics GmbH, Nonnenwald 2, D-82372 Penzberg, Germany*

Received April 14, 2003

## ABSTRACT

A method for biomolecular recognition is reported using light scattering of a single gold nanoparticle functionalized with biotin. Addition of streptavidin and subsequent specific binding events alter the dielectric environment of the nanoparticle, resulting in a spectral shift of the particle plasmon resonance. As we use single nanoparticles showing a homogeneous scattering spectrum, spectral shifts as small as 2 meV can be detected.

Biomolecular recognition has become an indispensable tool in clinical diagnostics as well as in pharmacology. Practically all relevant recognition schemes rely on specific biomolecular recognition reactions. Several techniques are in use today to monitor molecular binding events, including radioactive labeling, as well as chemical and optical detection. Even though each of these techniques has its own strengths and limitations, for many applications optical assays are the method of choice.

In this letter we present a method for specific biomolecular detection based on light scattering spectroscopy of single gold nanoparticles. Sub-wavelength sized noble metal nanoparticles show a pronounced resonance in their scattering spectrum for visible light. This nanoparticle plasmon (NPP) resonance can be tuned over a wide spectral range by changing intrinsic parameters such as the nanoparticle's material, its size, or its geometrical shape.<sup>1,2</sup> Even more importantly, extrinsic parameters such as the dielectric properties of the particle's immediate environment (nano-environment) or charge distributions decisively influence the NPP resonance position.<sup>1,3</sup> For a 40 nm sized nanoparticle, the resonance is sensitive only to the refractive index 10 to 20 nm above the nanoparticle's surface. Only a change of refractive index inside this nanoenvironment should lead to a significant shift of the NPP resonance spectrum.

Biomolecular binding events close to the surface of a noble metal nanoparticle may increase the refractive index of the nanoparticle's immediate environment and subsequently cause a red shift of the homogeneous NPP resonance. Accordingly, one of the binding partners has to be attached to the surface of the gold nanoparticle, i.e., the nanoparticle has to be functionalized. Our assay proposal is based on changing and measuring the spectrum of an *individual* nanoparticle. This is conceptually different from other assays utilizing noble metal nanoparticles, as they either rely on determining the amount of bound gold nanoparticles,<sup>4–7</sup> use coupled particle plasmon oscillations,<sup>8–11</sup> or rely on large ensembles of nanoparticles.<sup>12,13</sup> Recent studies use two-dimensional arrays of noble metal nanoparticles to detect molecules of high molecular weight,<sup>14</sup> or the measurements are carried out in nitrogen atmosphere.<sup>15</sup> For those cases, the spectral changes are sufficiently large to be detected in ensemble measurements. A single nanoparticle assay, however, should be sensitive enough to detect spectral shifts of only a few meV, which would be caused, e.g., by lower molecular weight molecules under physiological conditions. Single metal nanoparticle spectroscopy has been successfully demonstrated by using near-field scanning optical,<sup>16</sup> total internal reflection,<sup>17</sup> and dark-field microscopy.<sup>2,4</sup> Important further advantages of *single*-nanoparticle sensors are that in principle only a small absolute number of analyte molecules are used and that they feature the possibility of miniaturization and hence massive parallelization.

\* Corresponding author. E-mail: gunnar.raschke@physik.uni-muenchen.de  
<sup>†</sup> Present address: Lawrence Berkeley National Laboratory, Hildebrand Hall Box 101, Berkeley, CA 94720.

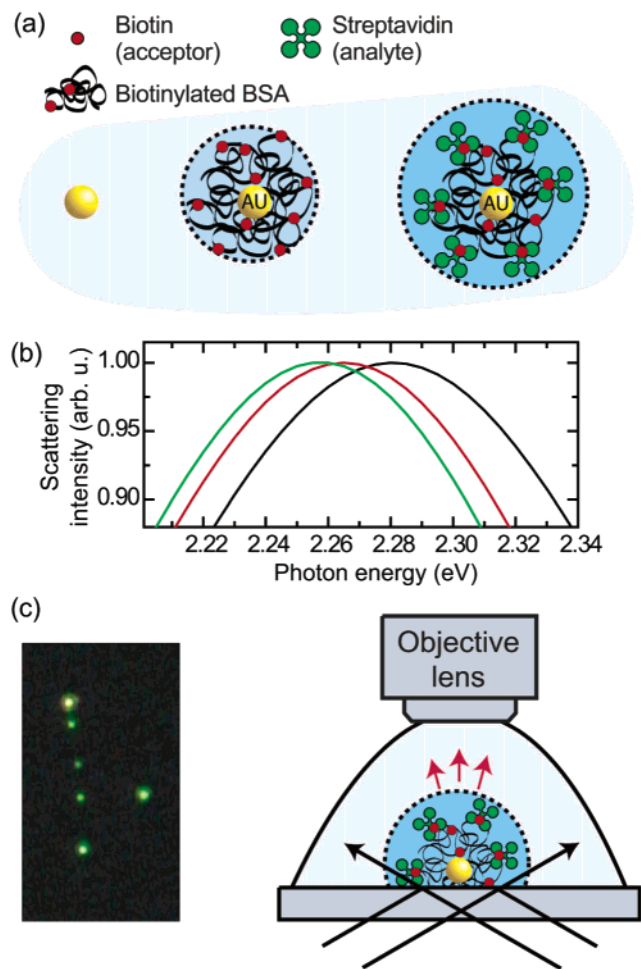


**Figure 1.** Principle and schematic representation of a biosensor based on light scattering from a single gold nanoparticle. (a) Single gold nanoparticles are functionalized with biotinylated BSA which subsequently binds streptavidin. (b) Mie theory calculations for the three different environments shown in (a). (c) Left: true color photograph of a sample of functionalized gold nanoparticles in dark-field illumination. Right: experimental setup facilitating dark-field microscopy of single gold nanoparticles immersed in liquids.

Figure 1a shows conceptually how protein binding events cause a change in refractive index of the nanoenvironment of a gold nanoparticle. In our model the refractive index gradually changes from that of a buffer solution ( $n = 1.33$ ) in the case of bare nanoparticles, over a 3 nm thick shell of higher refractive index after functionalizing the nanoparticles with acceptor molecules, to an increased 5 nm shell of high refractive index upon analyte binding (Figure 1a). Using Mie theory<sup>18</sup> we have calculated the scattering spectra for these three cases assuming a refractive index of  $n = 1.5$  for proteins (Figure 1b). This calculation predicts that the NPP resonance of an uncoated nanoparticle (Figure 1b, black curve) shifts 16 meV to the red as a result of functionalization (Figure 1b, red curve) and by another 7.5 meV upon formation of a complete shell of analyte molecules (Figure 1b, green curve).

In Figure 1c the scattered light from single individual functionalized gold nanoparticles of 40 nm diameter, electrostatically attached on a cover slip, can be seen with the naked eye in a dark-field microscope setup. White light from

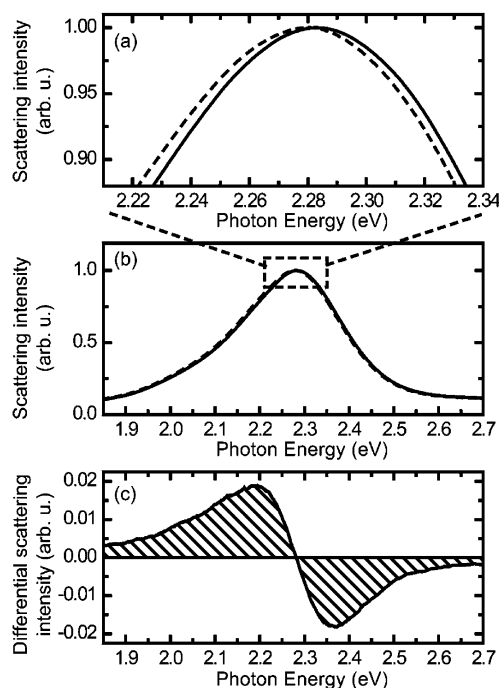


**Figure 2.** Spectroscopic detection of streptavidin binding to a single gold nanoparticle functionalized with biotin-BSA. (a, b) Comparison of experimental NPP resonance spectra in buffer before (solid line) and 30 min after adding streptavidin (dashed line). (c) Differential spectrum of the two scattering spectra shown in (b).

a 100 W halogen lamp is focused under large angles onto the sample using a dark-field condenser with high numerical aperture ( $NA = 1.2-1.4$ ). As depicted in Figure 1c, the scattered light of a single nanoparticle in focus can be collected by a water immersion objective lens ( $100\times$ ,  $NA = 1.0$ ), spectrally resolved in a grating spectrometer, and detected with a nitrogen-cooled and back-illuminated CCD camera. In the following we show that the NPP scattering resonance red shifts upon specific analyte binding.

First, the nanoparticles are functionalized with biotinylated bovine serum albumin (biotin-BSA) molecules (MW: 67 000 D). As analyte we use streptavidin (MW: 52 000 D), a tetrameric protein which can bind up to four biotin molecules. Biotin-BSA coated gold nanoparticles are immobilized onto the surface of a silanized glass substrate and covered by 10 mM Tris  $[\text{NH}_2\text{C}(\text{CH}_2\text{OH})_3]$ /BSA buffer solution (pH 8.0, 0.5 mg/mL BSA). Silanization together with BSA in the buffer solution is intended to prevent nonspecific streptavidin binding on the glass substrate and the objective lens. For an individual functionalized nanoparticle we find a scattering spectrum at a resonance position of 2.282 eV (Figure 2a,b, solid curve). To start the experiment, 10  $\mu\text{L}$  potassium phosphate buffer (pH 6.5, 20 mM) containing  $6 \times 10^{-5}$  mol/L streptavidin is added to a final streptavidin concentration of  $2 \times 10^{-6}$  mol/L. The assay is then incubated for 30 min. This results in a 5 meV spectral shift of the NPP resonance curve (Figure 2a,b, dashed curve) which is also clearly seen in the differential spectrum (Figure 2c). The shape of this differential scattering spectrum indicates that the addition of streptavidin induces a pure shift of the NPP resonance. The experimentally determined shift of 5 meV

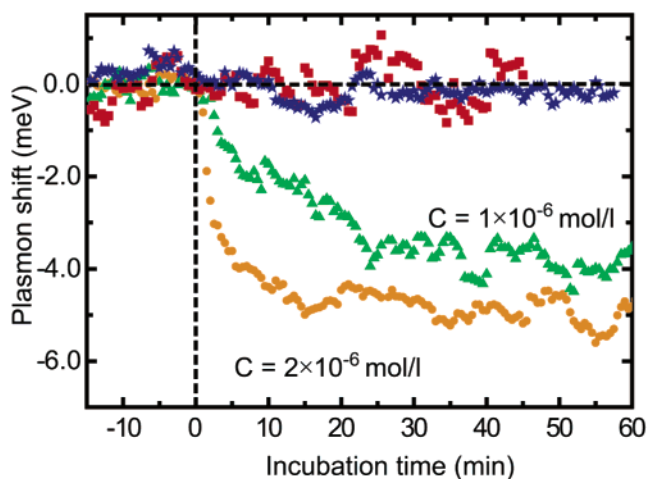


**Figure 3.** Resonance shift versus incubation time for different streptavidin concentrations and control experiments. Upon addition of streptavidin at time  $t = 0$  the NPP resonance starts to red shift (green triangles and orange circles), while addition of potassium phosphate storage buffer leaves the resonance position unchanged (red squares). The streptavidin concentration is  $1 \times 10^{-6}$  mol/L and  $2 \times 10^{-6}$  mol/L for triangles and circles, respectively. Addition of streptavidin to a final concentration of  $1 \times 10^{-6}$  mol/L to a nanoparticle coated with nonbiotinylated proteins shows no evidence for unspecific binding events (blue asterisks).

agrees well with the theoretically expected value of 7.5 meV for free nanoparticles in buffer solution. The difference can be easily explained by the fact that in the experiment the nanoparticles are not free, but attached to a substrate. Accordingly, one-third of the functionalized nanoparticle surface is not available for the analyte molecules.

To ensure that the observed red shift is not caused by the added potassium phosphate storage buffer of the streptavidin or due to unspecific binding, we perform supplementary control experiments. First, we monitor the resonance position of an individual nanoparticle coated with biotin-BSA in Tris/BSA buffer for 15 min (Figure 3, red squares). At  $t = 0$  min, 10  $\mu$ L of potassium phosphate buffer (equal to the streptavidin storage buffer) is added to the solution. Subsequent monitoring of the resonance position for additional 45 min does not show any shift, and hence buffer-induced changes of the nanoenvironment do not occur. In a second control experiment we use gold nanoparticles coated with nonbiotinylated proteins. This time, at  $t = 0$  min streptavidin is added to the Tris/BSA buffer up to a final concentration of  $1 \times 10^{-6}$  mol/L. As shown by the blue asterisks in Figure 3, no spectral shift occurs. We thus conclude that the observed red shift is a direct consequence of streptavidin binding.

Now we turn to the kinetics of the specific binding processes. At time  $t = 0$  min, 3.12 mg/mL streptavidin (corresponding to a molar concentration of  $6 \times 10^{-5}$  mol/L) is added to a Tris/BSA buffer solution (10 mM, pH 8.0, 0.5 mg/mL), resulting in a final streptavidin concentration of 100  $\mu$ g/mL ( $2 \times 10^{-6}$  mol/L). One minute after streptavidin addition, the NPP resonance position exhibits a significant red shift (Figure 3, orange circles). It saturates with increasing incubation time and reaches a constant total

displacement of 5 meV after approximately 15 min. Data points plotted as green triangles in Figure 3 correspond to a lower concentration, where streptavidin is added at  $t = 0$  min to a final concentration of 50  $\mu$ g/mL ( $1 \times 10^{-6}$  mol/L). Compared to the higher concentration, the red shift evolves on a slower time scale and the total NPP shift is reduced.

In the following we show that the observed time behavior is governed by the kinetics of the binding reaction and is not limited by diffusion. The rate  $\Delta N/\Delta t$  of streptavidin molecules impinging onto a free nanoparticle due to diffusion is given by<sup>19</sup>  $\Delta N/\Delta t = 4\pi D r C$ , where  $D = 7.4 \times 10^{-7}$  cm<sup>2</sup>/s is the diffusion constant of streptavidin,<sup>20</sup>  $r = 23$  nm is the radius of a functionalized nanoparticle, and  $C = 1 \times 10^{-6}$  mol/L is the molar concentration of free streptavidin molecules. For diffusion-limited kinetics this rate would lead to a completely filled streptavidin shell around the functionalized nanoparticle in less than one second. Consequently, the observed time evolution of the NPP resonance shift is not determined by diffusion but by the kinetics of the binding reaction. For our data set we apply a first-order model for binding analyte molecules to acceptor sites.<sup>21</sup> The deduced affinity constant of  $K_a = 10^6$  L/mol is much lower than expected for free biotin-streptavidin binding. We attribute this low value to the fact that the biotin molecules are located within a disordered protein network of BSA molecules. This leads to limited accessibility of biotin molecules and thus lower association rates. In addition, the BSA matrix may cause enhanced dissociation of bound biotin-streptavidin complexes. Low association rates and enhanced dissociation rates due to surface effects lead to drastically reduced affinity constants.<sup>22</sup>

In conclusion, this study demonstrates a real-time biotin-streptavidin affinity biosensor using light scattering spectroscopy of single gold nanoparticles. We expect further improvements of the limit of detection by sharpening of the resonance peak as it can, in principle, be achieved by the use of nanorods instead of nanospheres.<sup>2</sup> Considering the tiny dimensions of a single nanoparticle, this type of assay provides the potential to miniaturize immunoassays down to the micron scale and parallelize them, e.g., in array formats for multiplex testing.

**Acknowledgment.** We thank M. Seitz and C. Effenhauser for fruitful discussions as well as A. Helfrich, D. Spahn, and W. Stadler for excellent technical assistance. Financial support by the Bayerische Forschungsförderung through the funding program For Nano is gratefully acknowledged.

## References

- (1) Kreibig, U.; Vollmer, M. *Optical Properties of Metal Clusters*; Springer: Berlin, 1995.
- (2) Sönnichsen, C.; Franzl, T.; Wilk, T.; von Plessen, G.; Feldmann, J.; Wilson, O.; Mulvaney, P. *Phys. Rev. Lett.* **2002**, *88*, 077402.
- (3) Mulvaney, P. *Langmuir* **1996**, *12*, 788.
- (4) Yguerabide, J.; Yguerabide, E. E. *Anal. Biochem.* **1998**, *262*, 157.
- (5) Schultz, S.; Mock, J.; Smith, D. R.; Schultz, D. A. *J. Clin. Ligand Assay* **1999**, *22*, 214.
- (6) Schultz, S.; Smith, D. R.; Mock, J. J.; Schultz, D. A. *Proc. Natl. Acad. Sci. U.S.A.* **2000**, *97*, 996.
- (7) Yguerabide, J.; Yguerabide, E. E. *J. Cell. Biochem. Suppl.* **2001**, *37*, 71.

- (8) Mirkin, C. A.; Letsinger, R. L.; Mucic, R. C.; Storhoff, J. J. *Nature* **1996**, *382*, 607.
- (9) Alivisatos, A. P.; Johnsson, K. P.; Peng, X.; Wilson, T. E.; Loweth, C. J.; Bruchez, M. P., Jr.; Schultz, P. G. *Nature* **1996**, *382*, 609.
- (10) Elghanian, R.; Storhoff, J. J.; Mucic, R. C.; Letsinger, R. L.; Mirkin, C. A. *Science* **1997**, *277*, 1078.
- (11) Park, S. J.; Lazarides, A. A.; Mirkin, C. A.; Letsinger, R. L. *Angew. Chem., Int. Ed. Engl.* **2001**, *40*, 2909.
- (12) Englebienne, P. *Analyst* **1998**, *123*, 1599.
- (13) Englebienne, P.; Hoonacker, A. V.; Verhas, M. *Analyst* **2001**, *126*, 1645.
- (14) Riboh, J. C.; Haes, A. J.; McFarland, A. D.; Yonzon, C. R.; Van Duyne, R. P. *J. Phys. Chem. B* **2003**, *107*, 1772.
- (15) Haes, A. J.; Van Duyne, R. P. *J. Am. Chem. Soc.* **2002**, *124*, 10596.
- (16) Klar, T.; Perner, M.; Grosse, S.; von Plessen, G.; Spirkl, W.; Feldmann, J. *Phys. Rev. Lett.* **1998**, *80*, 4249.
- (17) Sönnichsen, C.; Geier, S.; Hecker, N. E.; von Plessen, G.; Feldmann, J.; Ditzbacher, H.; Lamprecht, B.; Krenn, J. R.; Aussenegg, F. R.; Chan, V. Z. H.; Spatz, J. P.; Moller, M. *Appl. Phys. Lett.* **2000**, *77*, 2949.
- (18) Bohren, C.; Huffmann, D. *Absorption and scattering of light by small particles*; John Wiley & Sons: New York, 1983.
- (19) Goldstein, B.; Coombs, D.; He, X. Y.; Pineda, A. R.; Wofsy, C. J. *Mol. Recognit.* **1999**, *12*, 293.
- (20) Spinke, J.; Liley, M.; Schmitt, F. J.; Guder, H. J.; Angermaier, L.; Knoll, W. *J. Chem. Phys.* **1993**, *99*, 7012.
- (21) Hall, D. *Anal. Biochem.* **2001**, *288*, 109.
- (22) Jung, L. S.; Nelson, K. E.; Stayton, P. S.; Campbell, C. T. *Langmuir* **2000**, *16*, 9421.

NL034223+